Evolutionary Journal of the Linnean Society, 2025, **4**(**1**), kzaf020
https://doi.org/10.1093/evolinnean/kzaf020
Advance access publication 23 October 2025

OXFORD

Original Article

Rib remodelling in fossil insular dwarf and mainland elephants from Greece

Pauline Basilia[1,2,*], Justyna J. Miszkiewicz[3,4], George A. Lyras[5], Athanassios Athanassiou[6], Alexandra A.E. van der Geer[4]

[1]Australian Research Centre for Human Evolution, Griffith University, Brisbane 4111, Australia
[2]Interdisciplinary Studies, Institute of Arts and Sciences, Far Eastern University, Manila 1015, Philippines
[3]School of Social Science, University of Queensland, St Lucia, Queensland 4072, Australia
[4]Vertebrate Evolution, Development and Ecology, Naturalis Biodiversity Center, Leiden 2300 RA, The Netherlands
[5]Faculty of Geology and Geoenvironment, National and Kapodistrian University of Athens, Athens 15784, Greece
[6]Ministry of Culture, Ephorate of Palaeoanthropology–Speleology, Athens 11636, Greece

[*]Corresponding author. Australian Research Centre for Human Evolution, Griffith University, 170 Kessels Road, Nathan, Queensland 4111, Australia.
E-mail: p.basilia@griffith.edu.au

ABSTRACT

In the Mediterranean, during the Middle and Late Pleistocene, populations of straight-tusked elephants (*Palaeoloxodon antiquus*) evolved repeatedly and independently into endemic dwarf species on several islands, including *P. creutzburgi* on Crete (Greece). Here we test whether this body size reduction was accompanied by changes in bone remodelling. Bone histology of non-weight-bearing ribs was compared between Cretan dwarf ($N = 5$) and mainland *P. antiquus* ($N = 20$) specimens from Greece. Rib cortical bone in both elephant samples displayed dense Haversian bone with evidence of remodelling up to the periosteum. We adjusted osteon densities and area, and Haversian canal to osteon ratio by cortical width. Results were statistically significantly ($P < .01$) higher in *P. creutzburgi* than in *P. antiquus*. This suggests remodelling in the smaller ribs was characterized by larger and more numerous osteons than in *P. antiquus*. We interpret these findings as indicative of a bone metabolic adaptation to the insularity-driven reduction of body mass in *P. creutzburgi*. This is possibly a response to its need for deposition of a higher quantity of bone within osteons and through maintaining osteon numbers that are comparable to the mainland ancestor. We propose that despite the size reduction of the skeletal frame of *P. creutzburgi*, bone quantity was maintained at higher levels to ensure metabolic viability.

Keywords: *Palaeoloxodon antiquus; Palaeoloxodon creutzburgi;* Pleistocene proboscidean; bone histology; remodelling stages; osteon population; super osteon; palaeohistology; Island Rule; insular dwarfism

INTRODUCTION

Growth rates and life history trajectories can be estimated from osteohistological characteristics preserved in fossil bones (Chinsamy 1997, de Ricqlès 2011, Padian and Lamm 2013, Kolb *et al.* 2015a). Bone formation and remodelling produce bone structures that reflect ontogenetic stages such that bone tissue can be fast-forming (e.g. woven-fibred bone) and slow-forming (e.g. parallel-fibred bone) in younger mammals (Francillon-Vieillot *et al.* 1990, Stein and Prondvai 2014) (Fig. 1). Lines of arrested growth (LAGs) indicate a temporary cessation of bone growth, and the external fundamental system (EFS) documents bone growth completion (Francillon-Vieillot *et al.* 1990, Köhler *et al.* 2012) (Fig. 1). At later stages in their lifespan, large mammals have dense Haversian bone due to secondary remodelling (Castanet 2006, Köhler *et al.* 2012, Straehl *et al.* 2013) (Fig. 1). Haversian bone is formed through resorption by osteoclasts and bone deposition by osteoblasts (Lassen *et al.* 2017). These cells constitute the basic multicellular unit (BMU), which leaves behind circular longitudinal structures known as secondary osteons (hereafter 'osteons') (Parfitt 1994, Frost 2000). These osteons consist of a central Haversian canal surrounded by concentric lamellae, which are bordered by a cement line (Lassen *et al.* 2017). Haversian bone remodels continuously throughout adulthood, notably in long-lived mammals, including humans (Stout and Crowder 2011), fossil and extant deer (Kolb *et al.* 2015b, Miszkiewicz and van der Geer 2022), fossil hippopotamuses (Miszkiewicz *et al.* 2023),

Received 07 June 2025; revised 22 September 2025; accepted 04 October 2025

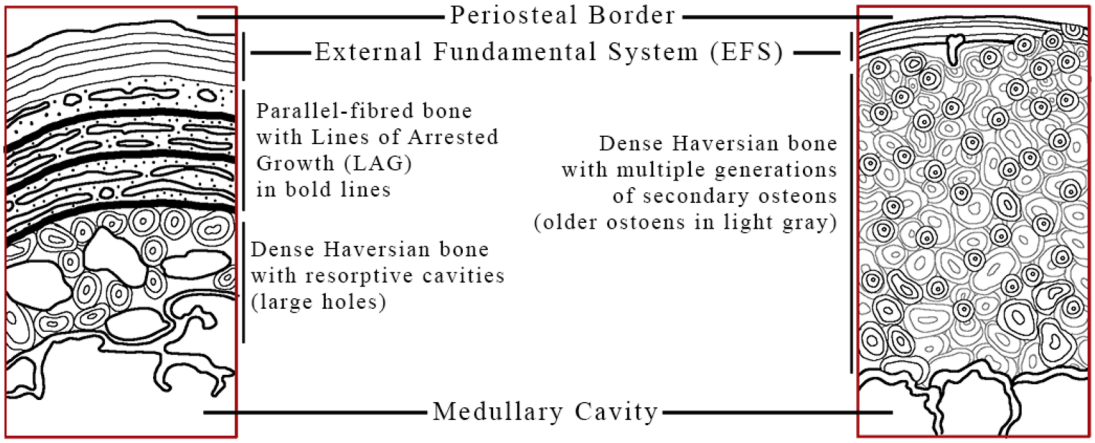

Figure 1. Schematic representations of microstructural features in mammalian cortical bone. Left: bone section showing histology in a young adult with the external fundamental system (EFS) at the periosteal border and lines of arrested growth (LAGs) in parallel-fibred bone tissue with dense Haversian bone at the endosteal layer. Right: bone section showing histology in an older individual with remodelling of the EFS at the periosteal region and widespread dense Haversian bone remodelling of cortical bone.

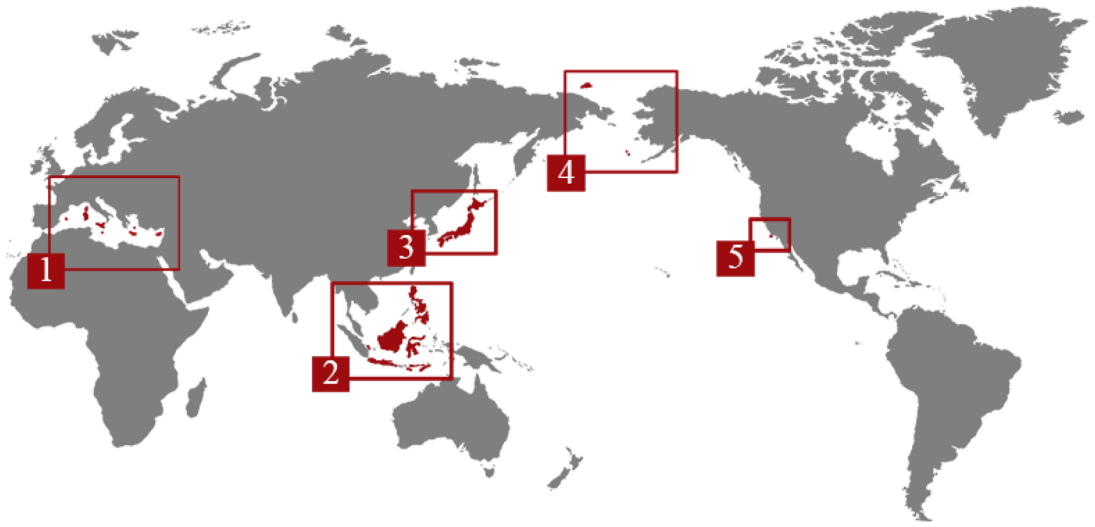

Figure 2. Insular proboscidean distribution worldwide: (1) the Mediterranean islands (subject of this study), (2) insular Southeast Asia, (3) Japan, (4) Arctic Islands, and (5) California Channel Islands. Data based on van der Geer *et al.* (2021).

bears (Wojda *et al.* 2013), extant and fossil Asian elephants (Ngan-vongpanit *et al.* 2017, Basilia *et al.* 2023c), and fossil stegodon (Basilia *et al.* 2023a).

Bone remodelling processes can be inferred from Haversian tissue by measuring variables such as: osteon population density (OPD), which represents the total amount of osteons formed in a given region of interest (ROI) of bone; osteon area (On.Ar), which represents bone area resorbed by osteoclasts; Haversian canal area (HCa.Ar), which reflects bone vascularity; and Haversian canal to osteon area ratio (HCa%), which is a measure of bone deposited within the osteon (Qiu *et al.* 2003, Skedros *et al.* 2013, Wojda *et al.* 2013). Remodelling can be influenced by many factors, e.g. age, sex, disease, mechanical variables, and microdamage repair (Thompson 1980, Bell *et al.* 2001, Havill 2004, Skedros *et al.* 2004, Britz *et al.* 2009, Lad *et al.* 2019). In mammals, less is known about the effect of insular dwarfism on Haversian bone and remodelling, although recent studies have reported retention of high remodelling with bone gain in a few insular dwarf mammals, e.g. in dwarf deer (Miszkiewicz and van der Geer 2022) and dwarf hippos (Miszkiewicz *et al.* 2023).

In this study, we examined bone histology in the large-sized straight-tusked elephant *Palaeoloxodon antiquus* (Falconer and Cautley, 1847) from mainland Greece, and its dwarfed descendant species, *Palaeoloxodon creutzburgi* (Kuss, 1965) from Crete (Fig. 2). Dwarf elephants are known from islands worldwide (Fig. 2), represented by several genera and species, and ranging from the middle Miocene to the early Holocene (van der Geer *et al.* 2021). The degree of dwarfism in insular dwarf species, including elephants, varies according to ecogeographical variables such as island geography, climate, time in isolation, number of ecologically relevant competitors, and predators (Lomolino *et al.* 2006, 2013, Lomolino 2016, van der Geer *et al.* 2016), following predictions according to the 'island rule' (Foster 1964, van Valen 1973, Lomolino 1985, Benítez-López *et al.* 2021). The Cretan elephant evolved a body mass decrease down to 38% of its ancestral body weight (Lomolino *et al.* 2013), weighing just over 3 metric tonnes,

compared to the around 8 metric tonnes of the mainland population. To characterize bone remodelling in this dwarf species in relation to that in its ancestral species without conflating multiple factors, we examined ribs which are not affected by biomechanical stimulation as much as limb bones (Waskow and Sander 2014, Basilia *et al.* 2023c).

Elephant bone histology

Surprisingly little is known about bone remodelling in the largest living land mammals—the African elephants (*Loxodonta africana*, *L. cyclotis*), and the Asian elephant (*Elephas maximus*). While histology in adults shows extensive Haversian bone (Nganvongpanit *et al.* 2017, Basilia *et al.* 2023c), extant juvenile elephants seem to lack Haversian bone in the first 2–3 years of lifespan (Curtin *et al.* 2012, Thitaram *et al.* 2018). Curtin *et al.*'s (2012) study on the histology of the tibia and femur of an *L. africana* neonate was one of the first osteohistological examinations of proboscidean post-cranial bones. Only woven bone was noted in the outer cortex, while woven bone and parallel-fibred bone, with primary osteons, were present in the inner cortex. Another study of two juvenile elephants (*E. maximus*) aged 2 years, and 2 years 9 months, found that cortical bone histology of their parietal bone consisted of primarily woven bone and plexiform bone, while the right humerus consisted of lamellar bone with primary osteons (Thitaram *et al.* 2018).

Some bone histology data have been published for Haversian bone in adult elephants. For example, osteons from adult extant elephants have been included in a study examining allometry of osteon size and body size across a range of mammals, finding that humeral and femoral osteons and body mass scale with negative allometry in large taxa (Felder *et al.* 2017). In adult female Asian elephants, histology of the humerus, radius, femur, tibia, fibula, and the fifth rib showed fully remodelled cortical bone with no evidence of younger or faster growing bone tissue (Nganvongpanit *et al.* 2017), confirming that bone growth slows down and experiences remodelling in adulthood. The data from Nganvongpanit *et al.* (2017) were compared to a Pleistocene Asian elephant from Indonesia within the same body size range (Basilia *et al.* 2023c). The fossil and extant data were similar, but the fossil rib displayed osteons with smaller areas, which was interpreted as reflecting differences in environmental stimuli that would have driven remodelling. Additionally, Basilia *et al.* (2023c, 2023a) reported the existence of various osteon variants, mirroring what was observed earlier in extant Asian elephants (Nganvongpanit *et al.* 2017), such as double cement lines and unusually large osteons measuring >100000 μm^2 (termed 'super osteons').

Factors determining Haversian remodelling, and the insular dwarf mammal context

Generally, prior mammalian bone histology research suggests that body size may influence geometric properties and densities of osteons (Felder *et al.* 2017, Miszkiewicz *et al.* 2020, Miszkiewicz and van der Geer 2022, Basilia *et al.* 2023b, Miszkiewicz *et al.* 2023), although this has not always been clear from the literature (Zedda and Babosova 2021). In a study on the effects of allometric scaling on femur and humerus bone histology from variously sized mammals (39 species with body mass ranging from 0.3 to 21000 kg), osteon infilling rates showed a negative allometry with body mass with larger species having smaller infill ratios for their body size (Felder *et al.* 2017). However, Zedda and Babosova (2021) reported a lack of a clear allometric scaling pattern between osteon measures and body mass within species when comparing histology of the humerus and the femur in cows and sheep. Zedda and Babosova (2021) concluded that, at least in these two taxa, lifestyle and biomechanics may play a more important role in determining aspects of bone histology than body mass per se. Apparently, and not surprisingly, interspecific scaling (evolutionary allometry) of osteons differs from intraspecific scaling (static allometry). Variation in osteon morphology and morphometry can also stem from ageing factors, such that compact bone that has been remodelled throughout lifespan reaches spatial capacity and adapts by altering osteon size (Takahashi *et al.* 1965). In other words, larger quantities of smaller osteons can be expected in bone tissue of advanced age since it had more time to accumulate them (Crowder 2016).

Dwarf elephants have more limited cortical bone in spatial terms than their larger mainland congeners in accordance with their smaller skeleton. Osteon variability may thus be constrained by available cortical space (Dominguez and Agnew 2016). This has been previously noted in the ribs of the crab-eating macaque (*Macaca fascicularis*) with narrow cortices (Lad *et al.* 2019), in large-sized sauropod dinosaurs (*Camarasaurus* sp.) where thinner rib cortices contained larger osteons (Waskow and Sander 2014), and in a dwarf proboscidean, *Stegodon florensis florensis*, of Flores (Basilia *et al.* 2023a). Therefore, decreasing/increasing body size and its associated reduction/increase of cortical bone space could have an influence on BMU activities and thus osteon morphometry. To date, only the study by Basilia *et al.* (2023a) examining *S. florensis* has characterized the histological aspects of cortical bone reduction on rib osteons in insular dwarf elephants. However, that study was limited by only examining one rib fragment that, additionally, showed widespread taphonomic damage obscuring bone histology. Here, we hypothesize that the smaller ribs of *P. creutzburgi* could potentially encourage the development of smaller osteons due to limited cortical space, and that the density of osteons would be higher for the small cortical space available reflecting active remodelling as has been previously reported for dwarf deer and dwarf hippopotamuses. We here compared *P. creutzburgi* with *P. antiquus* to assess how, and if, rib remodelling histological characteristics changed with body mass reduction.

MATERIALS AND METHODS

Palaeoloxodon rib samples

The *P. antiquus* specimens were recovered in 1902 at Issoma Karyon, Megalopolis Basin, Peloponnese, from a middle Pleistocene palaeolake site that yielded numerous fossiliferous deposits (Athanassiou *et al.* 2018) (Fig. 3A). All elephant remains from the entire basin belong to *P. antiquus* (Konidaris *et al.* 2018, Athanassiou 2021). Cut marks on a *P. antiquus* partial skeleton from a nearby site within the same palaeolake, Marathousa 1 (ca. 420–480 ka, Panagopoulou *et al.* 2018, Tourloukis *et al.* 2018), suggest butchering by hominins may have been performed on site.

The *P. creutzburgi* specimens originated from the upland Katharo Basin and the coastal cave area of Rethymnon province (Fig. 3B). The Katharo Basin is a 4-km-wide depression in the Dhikti

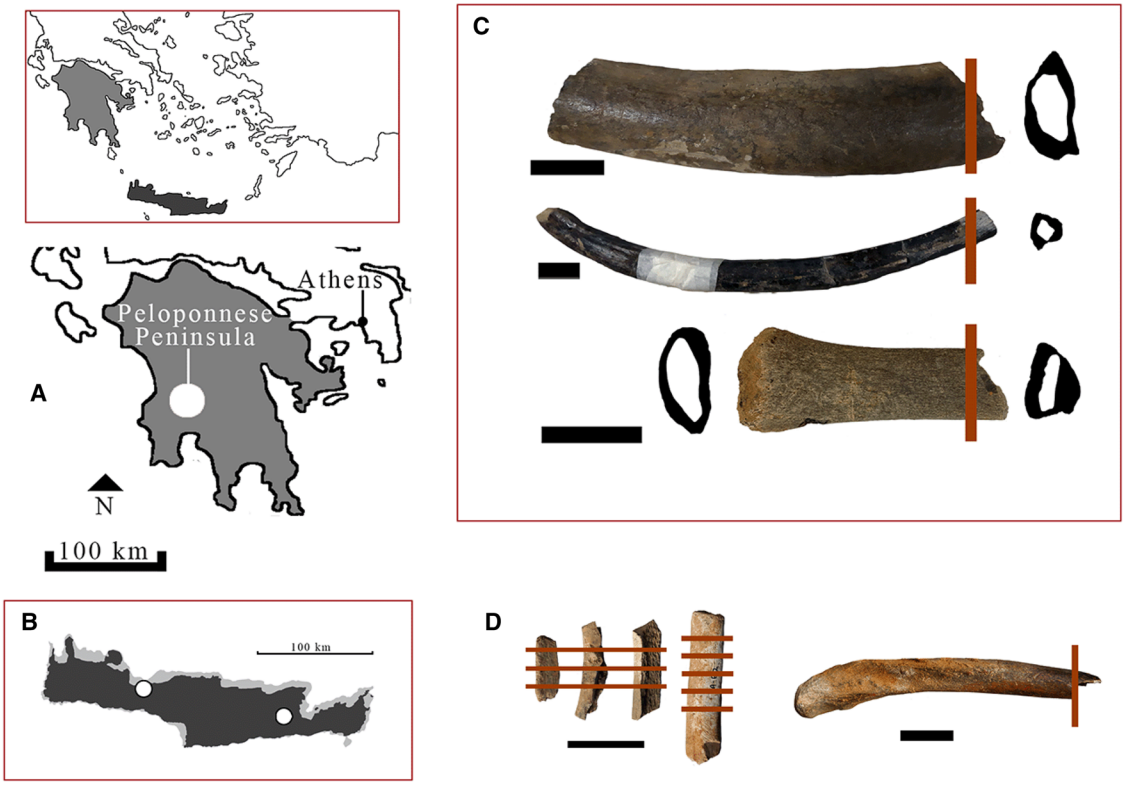

Figure 3. Map of Greece showing the Peloponnese peninsula (A) and Crete (B) indicating site locations of the mainland (*Palaeoloxodon antiquus*), white dot, and insular elephant species (*P. creutzburgi*), red dots, used in our study. Examples of fossil elephant specimens: C, *P. antiquus* specimens with cross-section schematic (from top) PA6, PA9, and PA22; and D, *P. creutzburgi* rib fragments (from left) PC1–PC4 from Katharo, and PC5 from Rethymnon. Red lines correspond to sampling locations. *Palaeoloxodon creutzburgi* samples from Katharo were sampled serially.

mountains, eastern Crete. There are several fossiliferous deposits here, informally referred to by the most common taxa, namely, the Deer Site, Hippo Site, and Elephant Site (Lyras *et al.* 2022). *Palaeoloxodon creutzburgi* specimens recovered from the Elephant site are mostly fragmentary, while those from coastal caves in the Rethymnon area show better preservation.

We sampled a total of 25 rib specimens, 20 *P. antiquus* (Fig. 3C) and five *P. creutzburgi* (Fig. 3D), in this study. All fossils derived from disarticulated and commingled assemblages making accurate identification of individuals impossible. The majority of ribs were fragmented, but it was possible to determine some basic anatomical identification of each rib (Table 1; for details see Supporting Information Table S1).

Histology procedures

To prepare thin sections we followed the same protocol for all specimens (see Miszkiewicz *et al.* 2019, 2020, Miszkiewicz and van der Geer 2022, Basilia *et al.* 2023c), but our procedures had to be conducted in different laboratories due to facility closures resulting from COVID-19 pandemic restrictions in Australia. However, the sample preparation and analysis were completed by the same two researchers (PB and JJM) ensuring consistency in the application of the same protocol. The samples were prepared at the Histology Laboratory of the School of Archaeology and Anthropology at the Australian National University (ANU, Canberra), and the Palaeontology Laboratory of the Australian Research Centre for Human Evolution at Griffith University (GU, Brisbane). The thin sections were imaged using facilities in the Biological Anthropology Research Laboratory (of the same ANU School), and in the Microscopy Laboratory of the School of Social Science at the University of Queensland (Brisbane).

The fossil specimens were documented pictorially prior to sample extraction for histology. Using a Dremel electric drill equipped with a carbon rotary blade, approximately 2-cm-thick bone sections were removed from each rib fragment. All extracted sections were embedded in epoxy resin and cut on a diamond blade of a low-speed precision saw (Kemet Micracut 151) in a transverse plane so that cortical bone histology surfaces could be revealed. The cut segment from each embedded block with the revealed surface was then glued on to a microscope slide using epoxy glue. Once mounted, the slides were ground on a series of grinding pads with various coarseness (400–1200 grit size). Once the slides were ground down to approximately 100 μm, they were polished and washed in an ultrasonic cleaner, dehydrated in a series of ethanol solution baths, cleared using xylene, and cover-slipped using DPX glue. The samples prepared at the ANU were imaged using an Olympus BX53 microscope and a DP74 camera. ROIs were captured using a 40× objective resulting in images approximately 1.78 mm high and 1.11 mm wide. The samples prepared at GU were imaged using an Olympus BX60 with a Michrome 5 Pro camera attachment. ROIs were captured using a 50× objective resulting in images approximately 1.6 mm high and 1.34 mm wide.

Table 1. *Palaeoloxodon antiquus* and *P. creutzburgi* rib fragments examined in this study, with anatomical remarks regarding external morphology, and sampling locations and description.

Specimen ID	Remarks on the anatomical appearance of each rib fragment prior to extracting samples for histology	Sample locations with description of cross-section following sampling
***Palaeoloxodon antiquus* (Megalopolis Basin)**		
PA1	Right proximal rib, vertebral rib with partial neck and narrow groove, flat morphology, complete cross-section with infilled medullary cavity	Ventral end, incomplete cross-section
PA3	Left distal rib, sternal rib with shallow groove, triangular morphology, complete cross-section with infilled medullary cavity	Medial surface, incomplete cross-section
PA4	Left proximal rib, vertebral rib with partial neck and deep groove, triangular morphology complete cross-section with infilled medullary cavity	Dorsal end, incomplete cross-section
PA5	Right proximal rib, vertebral rib with narrow groove, triangular morphology, complete cross-section with infilled medullary cavity	Ventral end, incomplete cross-section
PA6	Right distal rib, sternal rib with shallow groove, flat morphology, complete cross-section with infilled medullary cavity	Ventral end, incomplete cross-section
PA7	Right distal rib, sternal rib with deep groove, flat morphology, complete cross-section with infilled medullary cavity	Ventral end, incomplete cross-section
PA8	Left distal rib, sternal rib with shallow groove, flat morphology, complete cross-section with infilled medullary cavity	Ventral end, incomplete cross-section
PA9	Left partial proximal to distal rib, partial vertebral rib to sternal rib with deep groove, triangular morphology, complete cross-section, filled medullary space	Ventral end, incomplete cross-section
PA14	Left distal rib, sternal rib with shallow groove, flat morphology, complete cross-section with infilled medullary cavity	Ventral end, incomplete cross-section
PA15	Right distal rib, vertebral rib with shallow groove, flat morphology, complete cross-section with infilled medullary cavity	Ventral end, incomplete cross-section
PA16	Right diaphysis of proximal to distal rib, vertebral rib with shallow bilateral groove, flat morphology, complete cross-section, infilled medullary cavity	Ventral end, incomplete cross-section
PA17	Left proximal rib, vertebral rib with shallow groove, rounded morphology, complete cross-section with infilled medullary cavity	Ventral end, incomplete cross-section
PA18	Left distal rib, vertebral rib with shallow groove, flat morphology, complete cross-section with infilled medullary cavity	Ventral end, incomplete cross-section
PA20	Right rib fragment, partial vertebral rib to sternal rib with shallow groove, flat morphology	Ventral end, complete cross-section combined from separate slides
PA21	Right proximal rib, vertebral to sternal rib with shallow groove, complete cross-section, rounded morphology, infilled medullary cavity	Ventral end, incomplete cross-section
PA22	Distal rib end, sternal rib end, complete cross-section with infilled medullary cavity from distal end	Dorsal end, incomplete cross-section
PA23	Indeterminate rib fragment, incomplete cross-section	Lateral surface, incomplete cross-section
PA24	Indeterminate rib fragment, incomplete cross-section	Lateral surface, incomplete cross-section
PA25	Indeterminate rib fragment, incomplete cross-section	Lateral surface, incomplete cross-section
PA26	Indeterminate rib fragment, incomplete cross-section	Lateral surface, incomplete cross-section
Palaeoloxodon creutzburgi		
PC1	Indeterminate rib fragment, incomplete cross-section; Elephant Site, Katharo	Serial sampling of whole sample, incomplete cross-section
PC2	Indeterminate rib fragment, incomplete cross-section; Elephant Site, Katharo	Serial sampling of whole sample, incomplete cross-section
PC3	Indeterminate rib fragment, incomplete cross-section; Elephant Site, Katharo	Serial sampling of whole sample, incomplete cross-section
PC4	Right distal rib, vertebral rib with shallow bilateral groove, complete cross-section with infilled medullary cavity; Elephant Site, Katharo	Serial sampling of whole sample, complete cross-section
PC5	Left proximal rib (neck, without head and tuberculum), vertebral rib, complete cross-section with infilled medullary cavity from distal; unknown cave site, Rethymnon region	Distal end, incomplete cross-section

Specimens were recovered from a skeletally mixed but single-species assemblage. All *P. antiquus* specimens were recovered from the site Issoma Karyon in Megalopolis Basin of southern Greece. The *P. creutzburgi* specimens were recovered from the 'Elephant site' at the Katharo Basin and coastal caves of Rethymnon area of Crete. We were unable to extract complete cross-sections for most of the specimens due to heavy fragmentation of cross-sections after sample extraction. Sample blocks became fragmented upon extraction. Macro-images of sample blocks from non-serialized sampling are given in Supporting Information Table S4.

All images were scaled down to one size (1.6 mm height and 1.11 mm width) and magnification in Fiji/ImageJ 1.53t (Schindelin *et al.*, 2012). The ROIs were consistently captured in a series following the periosteal border and into the mid-cortex in both species. However, with *P. antiquus* having larger cross-sections than those of *P. creutzburgi*, there will be some small unavoidable variation in the bone region sampled. A total of 325 ROIs were analysed in this study, with a total of 193.7 mm^2 imaged for

histology for *P. creutzburgi* and 383.83 mm^2 for *P. antiquus*. For osteon parameters, a total of 514 and 1431 osteons with paired Haversian canals were measured in *P. creutzburgi* and *P. antiquus*, respectively.

Remodelling stages

We used techniques developed in dinosaur studies (Mitchell *et al.* 2017) to estimate remodelling stages (RS), which originally involve a three-step process: dividing the cortical area, counting osteon generations, and assigning remodelling stages. Mitchell *et al.* (2017) recommend to divide cortical area into three segments (inner, mid-, and outer cortex) as the most advanced remodelling occurs in the outer cortex, but our study only includes observations from the mid-cortex and outer cortex due to taphonomic alterations, i.e., discoloration and fragmentation, in the inner cortex of most specimens. Osteon generations were counted from overlapping osteons with the most remodelled, or 'bottom layer', osteons representing the first or oldest generation, and the intact, or 'top', osteons representing the last or youngest generation (Fig. 4A). The RS assignments starting at the subperiosteal cortex are RS 4 with one generation, and RS 14 with five generations. Since we did not distinguish between mid-cortex and outer cortex, we present the RS range (e.g. RS 7–9) instead. The RS reported here is the average from three repeated observations.

Bone histomorphometric variables

All bone histomorphometric procedures were completed in Fiji/ImageJ. Bone histomorphometry nomenclature used in this study follows recommended standards (Dempster *et al.* 2013). Prior to applying quantitative histology methods, each thin section was evaluated for bone tissue types to note whether Haversian bone was present and thus warrant research into bone remodelling parameters. All thin sections were almost entirely remodelled, and so standard cortical bone histology variables (Table 2) were examined in each ROI. The variables OPD, On.Ar, and HCa.Ar (Fig. 4B–D) were manually measured using a WACOM digital drawing tablet and stylus once each histology image had been imported into Fiji/ImageJ. For some ribs, we had several thin sections available for examination, so the OPD values are a mean calculated from multiple slides. Osteons with 90% of the cement line showing were considered intact osteons, while osteons obstructed by subsequent remodelling were considered fragmentary. Only osteons with a full Haversian canal within the image border were counted. Osteon (lamellar bone) wall thickness (B.Ar) and the percentage ratio of B.Ar (Fig. 4E) were two derived variables measuring bone area deposited in each remodelling event.

Statistical analyses

Since we cannot determine if the rib fragments belonged to different individuals, we can only compare overall bone remodelling data between the two species. To adjust for scaling effects caused by the body mass difference between the two species (3063 kg versus 7976 kg; Lomolino *et al.* 2013) on bone histology parameters, all histology variables were corrected by cortical width (Ct. Wi, Supporting Information Table S1), which was measured directly from slides. We present the mean value of three repeated measurements of the same histomorphometric variable. We used a non-parametric Mann–Whitney U test to account for unequal sample size to compare the two species using the open-access statistics software package PAST Palaeontological Statistics v.4.05 (Hammer *et al.* 2001), with $P \leq .05$ signifying statistical

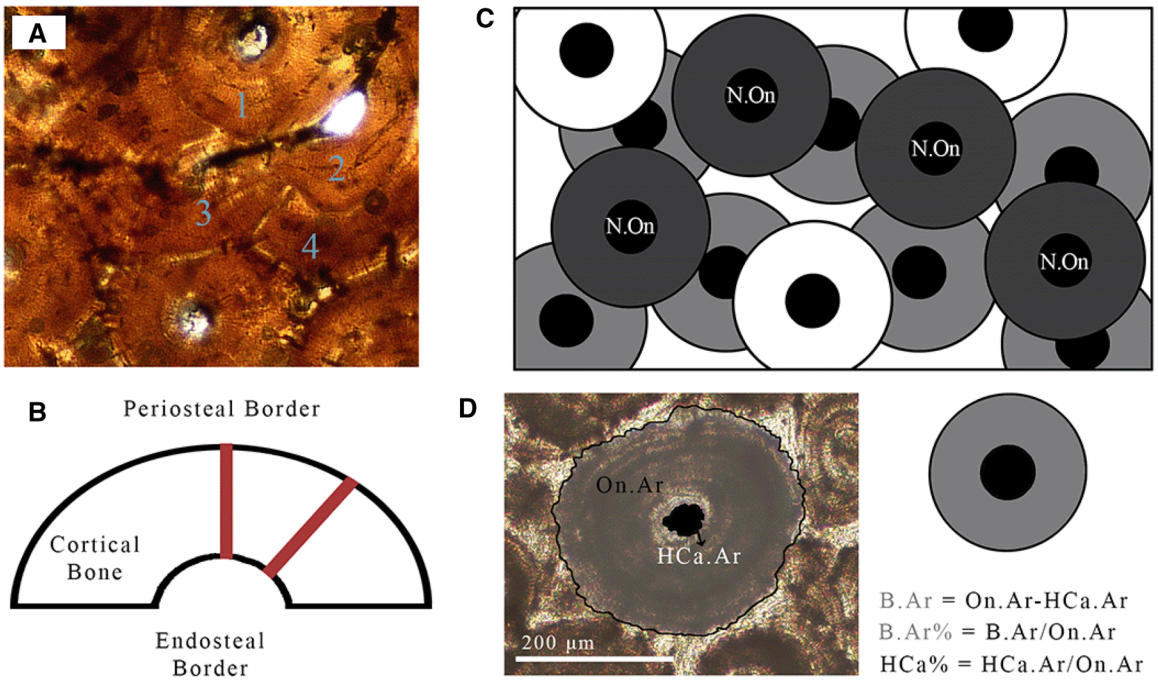

Figure 4. A, visualization of counting osteon generations for remodelling stages (RS); and B, schematic of cortical width measurement. Schematic representation of histomorphometric variables: C, osteon population density (OPD) through counting intact (N.On) and fragmentary osteons; D, left, osteon area (On.Ar) and Haversian canal area (HCa.Ar); and D, right, osteon wall area (B.Ar) and Haversian canal ratio (HCa%).

Table 2. Summary of bone histomorphometric variables examined in the present study.

Bone histomorphometric variable	Abbreviation	Definition
Remodelling stages	RS	Remodelling stages correspond to the combined number of osteon generations in the mid- and outer cortical region. Each generation was determined by counting the number of overlapping osteons, wherein the highest observed number of overlapping osteons is recorded (Fig. 4A) (following Mitchell *et al.* 2017).
Cortical width (mm)	Ct.Wi	Measured using the 'Straight Line' tool in Fiji/ImageJ; mean distance between the minimum and maximum width of cortical bone from the periosteal to endosteal border (Fig. 4B).
Osteon population density (OPD/mm²)	OPD	Total intact with total fragmentary osteons divided by the total ROI area (mm²) (Fig. 4C) (following Wojda *et al.* 2013).
Osteon area (On.Ar, µm²)	On.Ar	Only mature (i.e. completed) intact osteons measured for On.Ar by manually tracing the cement line using the 'Freehand' tool in Fiji/ImageJ (Fig. 4D).
Haversian canal area (HCa.Ar, µm²)	HCa.Ar	The outermost perimeter of the Haversian canal area for HCa.Ar (Fig. 4D) measured using the 'Freehand' Fiji/ImageJ tool.
Bone area (µm²)	B.Ar	HCa.Ar—On.Ar (Fig. 4E) (following Qiu *et al.* 2003)
Bone area ratio	HCa%	HCa.Ar/On.Ar (Fig. 4E) (following Qiu *et al.* 2003)

significance. We first provide general comments on qualitative bone histology, which is followed by results from quantitative analysis.

RESULTS

Cortical bone histology

The medullary cavity in the ribs of both *P. antiquus* and *P. creutzburgi* showed limited space and possibly infilling with (thickened trabecular) bone. Thin sections from both *P. antiquus* (Fig. 5A) and *P. creutzburgi* (Fig. 5B) had widespread Haversian bone with clear evidence for several generations of bone remodelling. Cortical remodelling near the periosteal border eradicated the EFS, so it was not visible in the thin sections. Parallel-fibred bone tissue was observed only in two *P. creutzburgi* specimens (PC2 and PC4, Fig. 5C), while circumferential lamellae in both taxa were restricted to the mid-cortical region. Parallel-fibred bone was identified in the cutaneous region of specimen PC4. Both species exhibited atypical osteon structures, including 'super osteons' (Fig. 5D, E), and double-zonal or embedded osteons (in the sense of Skedros *et al.* 2007) (Fig. 5F).

Remodelling stages

Haversian bone remodelling in the ROIs of the dwarf elephant had three to four osteon generations corresponding to RS 10–11 and RS 12–13. The mainland elephant had a wider range of osteon generations, from two generations to six generations corresponding to RS 7–15. Although there were few *P. antiquus* ($N = 4$) specimens that could be assigned to RS 12–13, dwarf and ancestor elephant ontogenetic stages fell within RS 10–11 (Supporting Information Table S2). Statistical comparison of the median osteon generation counts of the two elephant species ($U = 10719$, $P = .3769$) indicates that they share similar Haversian bone remodelling age (Fig. 6).

Differences in bone remodelling

The Ct.Wi measurements gave an average of 4.48 ± 1.15 mm for *P. creutzburgi* and 8.95 ± 4.2 mm for *P. antiquus*. We found differences in all of the histology variables between the two species ($P < .05$) (Table 3; see Supporting Information Table S3 for values without Ct.Wi correction). As illustrated in the violin plots (Fig. 6), the data were unequally distributed throughout all histomorphometric variables examined. The larger elephant consistently exhibited lower values compared with the dwarf elephant. Results of OPD comparison suggested there were more secondary osteons produced per mm² in *P. creutzburgi* for its rib size when compared to *P. antiquus*. Additionally, the dwarf elephant also produced resorption (On.Ar) and Haversian canals of a relatively large area for its rib size, but the infilling ratio (B.Ar and HCa%) had higher values for *P. creutzburgi* whereby its osteons had more bone within than in *P. antiquus*.

DISCUSSION

We found differences in Haversian bone remodelling between the dwarf *P. creutzburgi* and larger *P. antiquus* elephant ribs. The smaller rib bones from the dwarf elephant exhibited relatively larger osteons and higher osteon densities compared with the robust bones of its larger ancestor, but their remodelling stages were similar despite clear differences in body size. This finding partially met our prediction as we hypothesized smaller osteon area in *P. creutzburgi*. However, the bone area and percentage Haversian canal to osteon ratio showed that the smaller *P. creutzburgi* also had larger quantities of lamellar bone deposited within its osteons compared to *P. antiquus*. Our findings point to a pattern in rib bone remodelling of *P. creutzburgi* that was based around the need for deposition of a high quantity of bone relative to the size of its ribs.

The small ribs of the Cretan dwarf elephant having larger osteon density and geometry for its size differs from the findings of intra-specific studies where robust and slender bones are compared (Epelboym *et al.* 2012, Goldman *et al.* 2014, Lad *et al.* 2019). In these prior studies, cortical bone area correlated with osteon geometric variation, which suggests that our results do not relate to bone space influencing osteon size. The formation of osteons that have relatively large areas indicates prolonged osteoclastic activity that resorbs bone for subsequent infilling with bone by

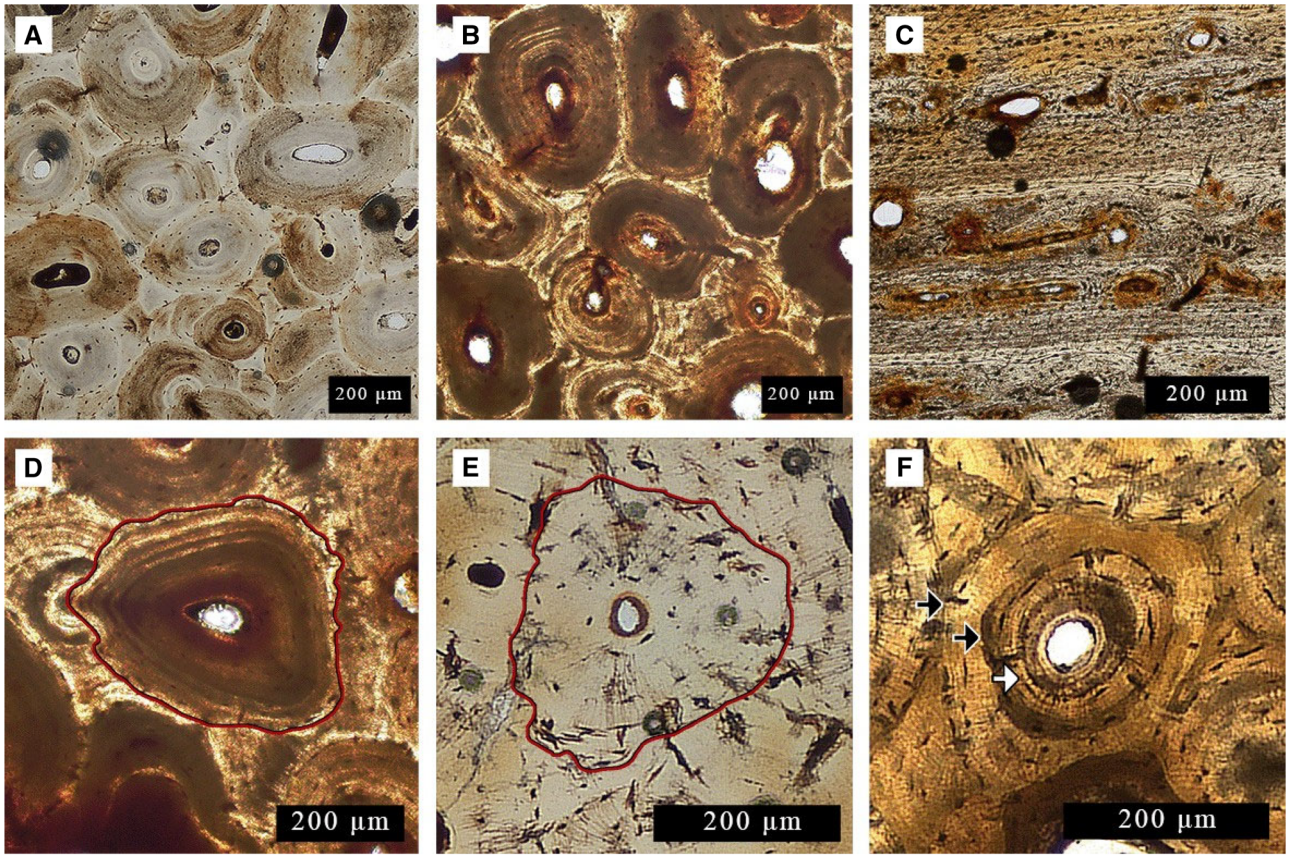

Figure 5. Examples of *P. antiquus* and *P. creutzburgi* bone histology: Haversian bone in (A) *P. antiquus* specimen PA9, and in (B) *P. creutzburgi* specimen, PC4; C, parallel-fibred bone in *P. creutzburgi*, PC4; atypical osteons, 'super osteons' with red line, in (D) *P. creutzburgi*, PC4, and in (E) *P. antiquus*, PA8; and F, embedded osteon with double-zoned osteon in *P. antiquus* specimen PA20. Black arrows indicate cement lines, while white arrow indicates cement line for latest remodelling.

Table 3. Results of histomorphometric analyses (mean ± SD) of *P. antiquus* and *P. creutzburgi* Haversian bone histology.

Bone histomorphometric variable	*P. antiquus*	*P. creutzburgi*	*U*	*P*
OPD	1.967 ± 0.88	3.205 ± 1.01	4531	<.01
On.Ar (µm²)	4.412 ± 3.43	12.331 ± 9.36	119000	<.01
HCa.Ar (µm²)	0.257 ± 0.30	0.831 ± 0.89	117000	<.01
B.Ar (µm²)	4.155 ± 3.28	11.500 ± 8.90	126130	<.01
H.Ca%	0.79 ± 0.55	1.87 ± 1.50	168220	<.01

All histomorphometric variables are unitless.

osteoblasts (Martin *et al.* 1980). If the amount of bone infilled was relatively small in relation to the area resorbed by osteoclasts this would have resulted in higher porosity of bone (through large Haversian canal areas) and thus a smaller total amount of bone available in the rib. Because our results for the ratio for osteon to canal area were statistically significantly higher in *P. creutzburgi* than in *P. antiquus*, it appears that the dwarf species had an advantage of having higher bone quantity deposited within osteons despite its smaller body and rib size. One of the key explanations for increased bone area within osteons cited in the biomedical literature is increased space for calcium exchange between bone and systemic circulation (Qiu *et al.* 2003, 2010). This is certainly a possibility in *P. creutzburgi*, but it would not explain why the ratio of osteon to canal space was smaller in *P. antiquus*. Since *P. antiquus* is the larger of the two taxa, calcium needs would probably be increased in a larger-bodied organism reflected in proportionally larger bone quantity within osteons. We do not have information about the sex of *P. creutzburgi* either, which could otherwise shed more light on possible elevated calcium requirements during periods of lactation or pregnancy (Athonvarangkul and Wysolmerski 2023). Another interpretation for increased calcium needs as inferred from large bone area could stem from dietary deficiencies. However, dietary deficiencies could also, in fact, link to lower osteon formation, which is not supported by our data, since adequate diet is needed to sustain healthy BMU processes (Paine and Brenton 2006, Cashman 2007). Furthermore, *P. creutzburgi* has been described as a 'generalist feeder' meaning it survived well on, and could adapt to, a range of foods in its environment without an indication that there might have been periodic shortages of resources (van der Geer *et al.* 2021) that could be linked to calcium deficiency. Differences between *P. creutzburgi* and *P. antiquus* in their bone remodelling indicators cannot be ascribed to age either because our RS results showed both specimens shared similar Haversian bone age, although we acknowledge that the fragmentary nature of the assemblage makes any age comparison tentative.

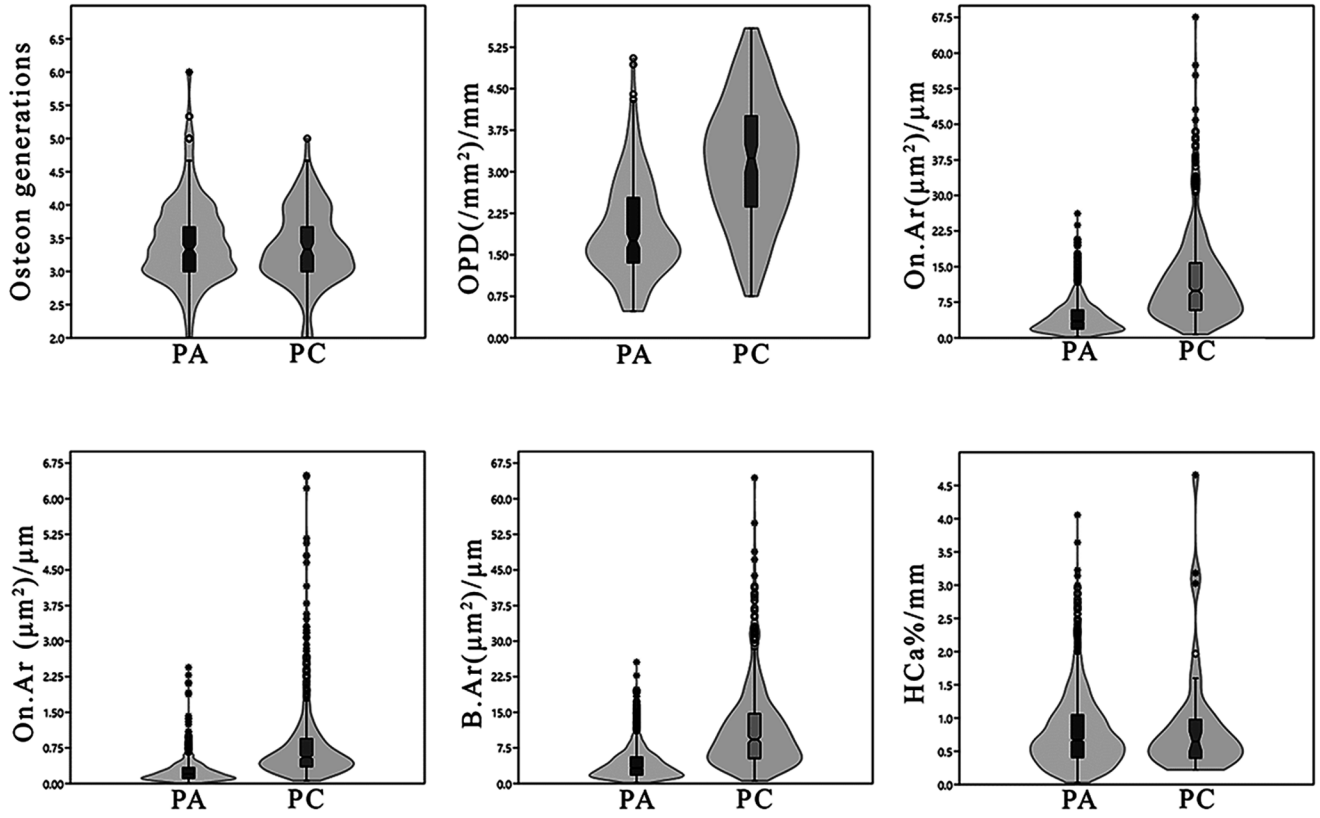

Figure 6. Comparison of bone histology data between *P. antiquus* (PA, green) and *P. creutzburgi* (PC, orange): osteon generation observations, osteon population density values (OPD/mm^2), osteon area (On.Ar, µm^2), Haversian canal area (HCa.Ar, µm^2), total bone area per osteon (B.Ar, µm^2), and percentage of Haversian canal per osteon (HC%) corrected. Bevel indicates mean value, while asterisk and circles are outliers.

It appears that the larger number of larger and denser (in terms of lamellar bone) osteons in *P. creutzburgi* when compared to *P. antiquus* is probably best explained by *P. creutzburgi*'s need for retention of higher bone quantity despite its skeletal frame reduction related to body size changes in an insular context. Similar observations have been made on ribs from other insular dwarf mammals, including the Cretan dwarf deer (*Candiacervus*) whose reduced body mass also correlated with a high density of osteons (Miszkiewicz and van der Geer 2022) and two species of dwarf hippopotamuses (*H. creutzburgi* from Crete, *H. minor* from Cyprus), which have increased osteocyte lacunae densities within osteons when compared with the much larger mainland hippopotamus *H. antiquus* (Miszkiewicz *et al.* 2023). For these three species, the reduction of body mass was proposed to have been accompanied by internal metabolic adaptations that include increased bone remodelling (bone gain dominating bone loss) to ensure skeletal homeostasis is maintained (Miszkiewicz and van der Geer 2022, Miszkiewicz *et al.* 2023). As our results here are similar, we propose that despite the size reduction of *P. creutzburgi*'s skeletal frame, bone quantity was maintained at higher levels to ensure metabolic viability (Doherty *et al.* 2015).

In terms of comparisons of the morphological appearance of histology in both taxa in our study, we found similarities that indicate some biological commonalities despite the body size differences. Both mainland and insular congeners had super osteons, previously described in extant Asian elephants (Nganvongpanit *et al.* 2017, Basilia *et al.* 2023c), insular fossil stegodon (Basilia *et al.* 2023a), and in insular fossil hippopotamus (Miszkiewicz *et al.* 2023). The presence of large osteons was hypothesized to be a product of extensive cortical area in large mammals (Basilia *et al.* 2023b). There was very little evidence remaining of the EFS due to advanced remodelling of the periosteal cortex, which, in combination with the RS data, is indicative of adulthood (Mitchell *et al.* 2017, Miszkiewicz and van der Geer 2022). However, some parallel-fibred bone tissue was identified in two of the *P. creutzburgi* specimens, with one (PC4) showing it clearly in the cutaneous region. Because growth in ribs is not asymptotic (Waskow and Sander 2014), the proximal part of the rib could show evidence for faster growing tissue, such as parallel-fibred bone, even if the distal part of the same rib already displays dense Haversian bone. Since PC2 and PC4 also showed advanced remodelling up until the periosteal border, indicating advanced age, similar to the rest of the specimens, the retention of parallel-fibred bone in this specimen may simply be a product of variation in the sampling location in our fragmented assemblage.

Both *P. creutzburgi* and *P. antiquus* showed evidence for trabecular infilling in the medullary cavity of their ribs, as was interpreted from minimal cavity seen in the samples. Infilling of the medullary cavity is a characteristic of limb bones in Asian elephants (Nganvongpanit *et al.* 2017), and in straight-tusked elephants, in which the medullary cavity in long limb bones occupies less than 1% of the total bone volume (Boschian *et al.* 2019). This infilling could be linked to mechanical needs in limb bones of graviportal taxa (Houssaye *et al.* 2016), but it might

serve a different purpose in elephant ribs. Semi-aquatic and, more evidently, aquatic mammals develop osteosclerosis, an increase in bone density through increased cortical thickness resulting in a decreased medullary cavity (Houssaye *et al.* 2016), to aid in buoyancy control (Larramendi & Height 2016). This may be advantageous for elephants, which can swim great distances (Johnson 1980). Osteosclerosis has indeed been previously noted in fossil proboscideans such as the insular dwarf Japanese *Stegodon aurorae* humerus with infilled medullary cavity and thickened cortex (Houssaye *et al.* 2016). Similar to the *Palaeoloxodon* ribs in our study, the ribs of Asian elephants (Nganvongpanit *et al.* 2017) and *Mammuthus primigenius* (Houssaye *et al.* 2016) also lacked open medullary cavities. The only way mainland *P. antiquus* could have migrated to Crete is through long-distance swimming as Crete was not connected to the mainland during the Pleistocene (Athanassiou *et al.* 2019). It may thus be that the osteosclerosis (infilled limb bones and ribs) was simply retained by the insular *P. creutzburgi* (infilled ribs) in the dwarfing process. Although the degree and location of osteosclerosis in proboscideans has yet to be fully documented, the lack of a medullary cavity in limb and rib bones of extant as well as extinct elephants seems to be a general, perhaps ancestral, pattern.

The main limitation of our study is the fragmented nature of the rib specimens, which are typical for thinner bones in the palaeontological record. There was also localized taphonomic damage which obscured some of the Haversian bone tissue limiting the availability of osteons for measurement. Furthermore, while we comment on a potential increase of calcium needs in our discussion, this is not supported by calcium content data or any processes of calcium metabolism in elephants. Also, we do not have any information on the individual age and sex of our specimens, so rely only on estimates of age from bone histology. Future research could include a histological analysis of elephant ribs from other geographical regions and temporal contexts across a range of juvenile and adult elephants to better characterize the change in bone remodelling with body size variation in elephants.

CONCLUSION

Our study provides important initial insights into the effects of insular dwarfing on Cretan elephants that may also occur in other insular dwarfed megaherbivores. We observed differences in bone histomorphometric variables between the Cretan dwarf elephant (*P. creutzburgi*) and the mainland form (*P. antiquus*), showing that the dwarf elephant's ribs contained higher densities of osteons that were filled with more bone than in the larger elephant. We interpret these findings as indicative of a bone metabolic adaptation to the reduction of body mass in *P. creutzburgi* to its need for deposition of a higher quantity of bone within osteons and through maintaining osteon numbers that are comparable to the mainland ancestor. We propose that despite the size reduction of *P. creutzburgi*'s skeletal frame, bone quantity was maintained at higher levels to ensure metabolic viability. Further, bone size reduction as a result of insular dwarfing might have also been accompanied by retention of osteosclerosis, a trait that may have been advantageous for its ancestor *P. antiquus*. Our study provides further evidence on insular adaptations of dwarfed megaherbivores at the bone microarchitecture level, adding to recently increasing data that there is a relationship between bone remodelling and body size reduction on islands.

ACKNOWLEDGEMENTS

We thank David McGregor and Kelvin Henderson for facilitating access to laboratory facilities at the Australian National University and the University of Queensland, and three anonymous reviewers for their helpful comments on the first version of this article.

AUTHOR CONTRIBUTIONS

Pauline Basilia (Conceptualization [Lead], Data curation [Equal], Formal analysis [Lead], Funding acquisition [Lead], Investigation [Equal], Methodology [Lead], Visualization [Equal], Writing—original draft [Lead]), Justyna J. Miszkiewicz (Conceptualization [Lead], Investigation [Equal], Methodology [Equal], Supervision [Equal], Writing—original draft [Equal], Writing—review & editing [Equal]), George A. Lyras (Resources [Lead], Visualization [Supporting], Writing—review & editing [Supporting]), Athanassios Athanassiou (Resources [Lead], Writing—review & editing [Equal]), and Alexandra van der Geer (Project administration [Lead], Resources [Lead], Supervision [Lead], Visualization [Lead], Writing—original draft [Equal], Writing—review & editing [Lead]).

SUPPLEMENTARY DATA

Supplementary data are available at *Evolutionary Journal of the Linnean Society* online.

CONFLICT OF INTEREST

None declared.

FUNDING

This study was funded through the Griffith University International Postgraduate Research Scholarship (to P. Basilia), the Australian Research Council (DE190100068; FT240100030 to J.J. Miszkiewicz) and Aspasia NWO 015.016.034 to A.A.E. van der Geer.

DATA AVAILABILITY STATEMENT

Data are available from figshare: https://doi.org/10.6084/m9.figshare.28553759

REFERENCES

Athanassiou A. The fossil record of continental elephants and mammoths (Mammalia: Proboscidea: Elephantidae) in Greece. In: *Fossil Vertebrates of Greece Vol. 1: Basal Vertebrates, Amphibians, Reptiles, Afrotherians, Glires, and Primates*. Berlin: Springer, 2021, 345-91.

Athanassiou A, van der Geer AAE, Lyras GA. Pleistocene insular Proboscidea of the Eastern Mediterranean: a review and update. *Quaternary Science Reviews* 2019;**218**:306–21.

Athanassiou A, Michailidis D, Vlachos E *et al.* Pleistocene vertebrates from the Kyparíssia lignite mine, Megalopolis Basin, S. Greece: Testudines, Aves, Suiformes. *Quaternary International* 2018;**497**:178–97.

Athonvarangkul D, Wysolmerski JJ. Crosstalk within a brain-breast-bone axis regulates mineral and skeletal metabolism during lactation. *Frontiers in Physiology* 2023;**14**:1121579.

Basilia P, Miszkiewicz JJ, Louys J *et al.* Insights into dwarf stegodon (*Stegodon florensis florensis*) palaeobiology based on rib histology. *Annales de Paléontologie* 2023a;**109**:102654.

Basilia P, Miszkiewicz JJ, Zaim J *et al.* Investigating super osteons in fossil Asian elephant (*Elephas maximus*) bone from Bangka Island, southeastern Sumatra. In: Louys J, Albers PCH, van der Geer AAE (eds.), *Quaternary Palaeontology and Archaeology of Sumatra*. Canberra, Australia: Australian National University Press, 2023b.

Basilia P, Miszkiewicz JJ, Nganvongpanit K *et al.* Bone histology in a fossil elephant (*Elephas maximus*) from Pulau Bangka, Indonesia. *Historical Biology* 2023c;**35**:1356–67.

Bell KL, Loveridge N, Reeve J *et al.* Super-osteons (remodeling clusters) in the cortex of the femoral shaft: Influence of age and gender. *The Anatomical Record* 2001;**264**:378–86.

Benítez-López A, Santini L, Gallego-Zamorano J *et al.* The island rule explains consistent patterns of body size evolution in terrestrial vertebrates. *Nature Ecology & Evolution* 2021;**5**:768–86.

Boschian G, Caramella D, Saccà D *et al.* Are there marrow cavities in Pleistocene elephant limb bones, and was marrow available to early humans? New CT scan results from the site of Castel di Guido (Italy). *Quaternary Science Reviews* 2019;**215**:86–97.

Britz HM, Thomas CDL, Clement JG *et al.* The relation of femoral osteon geometry to age, sex, height and weight. *Bone* 2009;**45**:77–83.

Cashman KD. Diet, nutrition, and bone health. *The Journal of Nutrition* 2007;**137**:2507S–12S.

Castanet J. Time recording in bone microstructures of endothermic animals; functional relationships. *Comptes Rendus Palevol* 2006;**5**:629–36.

Chinsamy A. Assessing the biology of fossil vertebrates through bone histology. *Paleontology of Africa* 1997;**33**:29–35.

Crowder CM. *Histological age estimation. Handbook of Forensic Anthropology and Archaeology.* London: Routledge, 2016, 222–35.

Curtin AJ, Macdowell AA, Schaible EG *et al.* Noninvasive histological comparison of bone growth patterns among fossil and extant neonatal elephantids using synchrotron radiation X-ray microtomography. *Journal of Vertebrate Paleontology* 2012;**32**:939–55.

de Ricqlès AJ. Vertebrate palaeohistology: past and future. *Comptes Rendus Palevol* 2011;**10**:509–15.

Dempster DW, Compston JE, Drezner MK *et al.* Standardized nomenclature, symbols, and units for bone histomorphometry: a 2012 update of the report of the ASBMR Histomorphometry Nomenclature Committee. *Journal of Bone and Mineral Research: The Official Journal of the American Society for Bone and Mineral Research* 2013;**28**:2–17.

Doherty AH, Ghalambor CK, Donahue SW. Evolutionary physiology of bone: bone metabolism in changing environments. *Physiology* 2015;**30**:17–29.

Dominguez VM, Agnew AM. Examination of factors potentially influencing osteon size in the human rib. *Anatomical Record (Hoboken, N.J.: 2007)* 2016;**299**:313–24.

Epelboym Y, Gendron RN, Mayer J *et al.* The interindividual variation in femoral neck width is associated with the acquisition of predictable sets of morphological and tissue-quality traits and differential bone loss patterns. *Journal of Bone and Mineral Research: The Official Journal of the American Society for Bone and Mineral Research* 2012;**27**:1501–10.

Felder AA, Phillips C, Cornish H *et al.* Secondary osteons scale allometrically in mammalian humerus and femur. *Royal Society Open Science* 2017;**4**:170431.

Foster JB. Evolution of mammals on islands. *Nature* 1964;**202**:234–5.

Francillon-Vieillot H, de Buffrénil V, Castanet J *et al.* Microstructure and mineralization of vertebrate skeletal tissues. In: Carter JG (ed.), *Skeletal Biomineralization: Patterns, Processes and Evolutionary Trends*, Vol. **1**. New York: Van Nostrand Reinhold, 1990, 471-530.

Frost HM. The Utah paradigm of skeletal physiology: an overview of its insights for bone, cartilage and collagenous tissue organs. *Journal of Bone and Mineral Metabolism* 2000;**18**:305–16.

Goldman HM, Hampson NA, Guth JJ *et al.* Intracortical remodeling parameters are associated with measures of bone robustness. *Anatomical Record (Hoboken, N.J.: 2007)* 2014;**297**:1817–28.

Hammer Ø, Harper DA, Ryan PD. PAST: Paleontological statistics software package for education and data analysis. *Palaeontologia Electronica* 2001;**4**:1–9.

Havill LM. Osteon remodeling dynamics in *Macaca mulatta*: normal variation with regard to age, sex, and skeletal maturity. *Calcified Tissue International* 2004;**74**:95–102.

Houssaye A, Waskow K, Hayashi S *et al.* Biomechanical evolution of solid bones in large animals: a microanatomical investigation. *Biological Journal of the Linnean Society* 2016;**117**:350–71.

Johnson DL. Problems in the land vertebrate zoogeography of certain islands and the swimming powers of elephants. *Journal of Biogeography* 1980;**7**:383–98.

Köhler M, Marín-Moratalla N, Jordana X *et al.* Seasonal bone growth and physiology in endotherms shed light on dinosaur physiology. *Nature* 2012;**487**:358–61.

Kolb C, Scheyer TM, Veitschegger K *et al.* Mammalian bone palaeohistology: a survey and new data with emphasis on island forms. *PeerJ* 2015a;**3**:e1358.

Kolb C, Scheyer TM, Lister AM *et al.* Growth in fossil and extant deer and implications for body size and life history evolution. *BMC Evolutionary Biology* 2015b;**15**:19–5.

Konidaris GE, Athanassiou A, Tourloukis V *et al.* The skeleton of a straight-tusked elephant (*Palaeoloxodon antiquus*) and other large mammals from the Middle Pleistocene butchering locality Marathousa 1 (Megalopolis Basin, Greece): preliminary results. *Quaternary International* 2018;**497**:65–84.

Lad SE, McGraw WS, Daegling DJ. Haversian remodeling corresponds to load frequency but not strain magnitude in the macaque (*Macaca fascicularis*) skeleton. *Bone* 2019;**127**:571–6.

Larramendi A, Height S. Body mass, and shape of proboscideans. *Acta Palaeontologica Polonica* 2016;**61**:537–74.

Lassen NE, Andersen TL, Pløen GG *et al.* Coupling of bone resorption and formation in real time: new knowledge gained from human Haversian BMUs. *Journal of Bone and Mineral Research: The Official Journal of the American Society for Bone and Mineral Research* 2017;**32**:1395–405.

Lomolino MV. Body size of mammals on islands: the island rule reexamined. *The American Naturalist* 1985;**125**:310–6.

Lomolino MV. The unifying, fundamental principles of biogeography: Understanding Island Life. *Frontiers of Biogeography* 2016;**8**.

Lomolino MV, Riddle BRC, Brown JHC. *Biogeography*. Sunderland, MA: Sinauer Associates, Inc; 2006.

Lomolino MV, van der Geer AA, Lyras GA *et al.* Of mice and mammoths: generality and antiquity of the island rule. *Journal of Biogeography* 2013;**40**:1427–39.

Lyras GA, Athanassiou A, van der Geer AA. The fossil record of insular endemic mammals from Greece. In: Vlachos E (ed.), *Fossil Vertebrates of Greece, Laurasiatherians, Artiodactyles, Perissodactyles, Carnivorans, and Island Endemics*, Vol. **2**. Cham: Springer, 2022, 661–701.

Martin RB, Pickett JC, Zinaich S. Studies of skeletal remodeling in aging men. *Clinical Orthopaedics and Related Research* 1980;268–82.

Miszkiewicz JJ, van der Geer AAE. Inferring longevity from advanced rib remodelling in insular dwarf deer. *Biological Journal of the Linnean Society* 2022;**136**:41–58.

Miszkiewicz JJ, Louys J, O'Connor S. Microanatomical record of cortical bone remodeling and high vascularity in a fossil giant rat midshaft femur. *Anatomical Record (Hoboken, N.J.: 2007)* 2019;**302**:1934–40.

Miszkiewicz JJ, Athanassiou A, Lyras GA *et al.* Rib remodelling changes with body size in fossil hippopotamuses from Cyprus and Greece. *Journal of Mammalian Evolution* 2023;**30**:1031–46.

Miszkiewicz JJ, Louys J, Beck RMD *et al.* Island rule and bone metabolism in fossil murines from Timor. *Biological Journal of the Linnean Society* 2020;**129**:570–86.

Mitchell J, Sander PM, Stein K. Can secondary osteons be used as ontogenetic indicators in sauropods? Extending the histological ontogenetic stages into senescence. *Paleobiology* 2017;**43**:321–42.

Nganvongpanit K, Siengdee P, Buddhachat K *et al.* Anatomy, histology and elemental profile of long bones and ribs of the Asian elephant (*Elephas maximus*). *Anatomical Science International* 2017;**92**:554–68.

Padian K, Lamm E-T. *Bone Histology of Fossil Tetrapods: Advancing Methods, Analysis, and Interpretation*. Berkeley, CA: University of California Press, 2013.

Paine RR, Brenton BP. Dietary health does affect histological age assessment: an evaluation of the Stout and Paine (1992) age estimation equation using secondary osteons from the rib. *Journal of Forensic Sciences* 2006;**51**:489–92.

Panagopoulou E, Tourloukis V, Thompson N *et al.* The lower Palaeolithic site of Marathousa 1, Megalopolis, Greece: overview of the evidence. *Quaternary International*, 2018;**497**:33–46.

Parfitt AM. Osteonal and hemi-osteonal remodeling: the spatial and temporal framework for signal traffic in adult human bone. *Journal of Cellular Biochemistry* 1994;**55**:273–86.

Qiu S, Fyhrie DP, Palnitkar S *et al.* Histomorphometric assessment of Haversian canal and osteocyte lacunae in different-sized osteons in human rib. *The Anatomical Record Part A: Discoveries in Molecular, Cellular, and Evolutionary Biology* 2003;**272**:520–5.

Qiu S, Rao DS, Palnitkar S *et al.* Dependence of bone yield (volume of bone formed per unit of cement surface area) on resorption cavity size during osteonal remodeling in human rib: implications for osteoblast function and the pathogenesis of age-related bone loss. *Journal of Bone and Mineral Research: The Official Journal of the American Society for Bone and Mineral Research* 2010;**25**:423–30.

Schindelin J, Arganda-Carreras I, Frise E *et al.* Fiji: an open-source platform for biological-image analysis. *Nature Methods* 2012;**9**:676–82. https://doi.org/10.1038/nmeth.2019

Skedros JG, Hunt KJ, Bloebaum RD. Relationships of loading history and structural and material characteristics of bone: development of the mule deer calcaneus. *Journal of Morphology* 2004;**259**:281–307.

Skedros JG, Sorenson SM, Jenson NH. Are distributions of secondary osteon variants useful for interpreting load history in mammalian bones? *Cells, Tissues, Organs* 2007;**185**:285–307.

Skedros JG, Knight AN, Clark GC *et al.* Scaling of Haversian canal surface area to secondary osteon bone volume in ribs and limb bones. *American Journal of Physical Anthropology* 2013;**151**:230–44.

Stein K, Prondvai E. Rethinking the nature of fibrolamellar bone: an integrative biological revision of sauropod plexiform bone formation. *Biological Reviews of the Cambridge Philosophical Society* 2014;**89**:24–47.

Stout SD, Crowder C. Bone remodeling, histomorphology, and histomorphometry. In: Crowder C Stout S (eds.), *Bone Histology: An Anthropological Perspective*. Boca Raton, FL: CRC Press, 2011, 17–38.

Straehl FR, Scheyer TM, Forasiepi AM *et al.* Evolutionary patterns of bone histology and bone compactness in xenarthran mammal long bones. *PLoS One* 2013;**8**:e69275.

Takahashi H, Epker B, Frost H. Relation between age and size of osteons in man. *Henry Ford Hospital Medical Journal* 1965;**13**:25–31.

Thitaram C, Matchimakul P, Pongkan W *et al.* Histology of 24 organs from Asian elephant calves (*Elephas maximus*). *PeerJ* 2018;**6**:e4947.

Thompson DD. Age changes in bone mineralization, cortical thickness, and haversian canal area. *Calcified Tissue International* 1980;**31**:5–11.

Tourloukis V, Muttoni G, Karkanas P *et al.* Magnetostratigraphic and chronostratigraphic constraints on the Marathousa 1 Lower Palaeolithic site and the Middle Pleistocene deposits of the Megalopolis basin, Greece. *Quaternary International*, 2018;**497**:154–69.

van der Geer AA, Lyras G, de Vos J *et al. Evolution of Island Mammals: adaptation and Extinction of Placental Mammals on Islands*. 2nd edn. Hoboken, NJ: Wiley-Blackwell, 2021.

van der Geer AA, van den Bergh GD, Lyras GA *et al.* The effect of area and isolation on insular dwarf proboscideans. *Journal of Biogeography* 2016;**43**:1656–66.

van Valen L. Patterns and the balance of nature. *Evolutionary Theory* 1973;**1**:31–49.

Waskow K, Sander PM. Growth record and histological variation in the dorsal ribs of *Camarasaurus* sp. (Sauropoda). *Journal of Vertebrate Paleontology* 2014;**34**:852–69.

Wojda SJ, Weyland DR, Gray SK *et al.* Black bears with longer disuse (hibernation) periods have lower femoral osteon population density and greater mineralization and intracortical porosity. *Anatomical Record (Hoboken, N.J.: 2007)* 2013;**296**:1148–53.

Zedda M, Babosova R. Does the osteon morphology depend on the body mass? A scaling study on macroscopic and histomorphometric differences between cow (*Bos taurus*) and sheep (*Ovis aries*). *Zoomorphology* 2021;**140**:169–81.